Int J Thermophys (2008) 29:1439–1456
DOI 10.1007/s10765-008-0501-2

Scattering of Thermal Waves and Non-steady Effective Thermal Conductivity of Unidirectional Fibrous Composites with Functionally Graded Interface

Xue-Qian Fang

Received: 5 March 2008 / Accepted: 21 July 2008 / Published online: 15 August 2008

Abstract In this paper, a thermal wave method is applied to investigate the non-steady effective thermal conductivity of unidirectional fibrous composites with a functionally graded interface, and the analytical solution of the problem is obtained. The Fourier heat conduction law is applied to analyze the propagation of thermal waves in the fibrous composite. The scattering and refraction of thermal waves by a cylindrical fiber with an inhomogeneous interface layer in the matrix are analyzed, and the results of the single scattering problem are applied to the composite medium. The wave fields in different material layers are expressed by using the wave function expansion method, and the expanded mode coefficients are determined by satisfying the boundary conditions of the layers. The theory of Waterman and Truell is employed to obtain the effective propagating wave number and the non-steady effective thermal conductivity of composites. As an example, the effects of a graded interface on the effective thermal conductivity of composites are graphically illustrated and analyzed. Analysis shows that the non-steady effective thermal conductivity under higher frequencies is quite different from the steady thermal conductivity. In the region of intermediate and high frequencies, the effect of the properties of the interface on the effective thermal conductivity is greater. Comparisons with the steady thermal conductivity obtained from other methods are also presented.

Keywords Fiber-reinforced composite materials · Functionally graded interface · Non-steady effective thermal conductivity · Scattering of thermal waves

X.-Q. Fang (✉)
Department of Engineering Mechanics, Shijiazhuang Railway Institute,
Shijiazhuang 050043, People's Republic of China
e-mail: fangxueqian@163.com

Nomenclature

λ	Thermal conductivity of the matrix
c	Specific heat capacity of the matrix
ρ	Mass density of the matrix
λ_0	Thermal conductivity of the fiber
c_0	Specific heat capacity of the fiber
ρ_0	Mass density of the fiber
a_0	Radius of fibers
a_{m-1}	Inner radius of each shell
a_m	Outer radius of each shell
h	Thickness of the interface
h_m	Thickness of each shell
C_l	Boundaries of the fiber and the shells
∇^2	Two-dimensional Laplacian operator
T	Temperature in composite materials
D	Thermal diffusivity
T_0	Average temperature
ω	Incident frequency of thermal waves
ϑ	Wave field of thermal waves
κ	Propagating wave number of thermal waves
k	Incident wave number
ϑ_0	Temperature amplitude of incident thermal waves
$J_m(\cdot)$	mth Bessel function of the first kind
$H_m^{(1)}(\cdot)$	mth Hankel function of the first kind
A_m, B_m, E_m, F_m	Mode coefficients
$H_m^{(2)}$	mth Hankel function of the second kind
$f_r(\theta)$	Far-field scattering amplitudes
K	Propagating wave number in the effective medium
N	Number of the fibers per unit volume
m	Total wave field in the matrix
V_f	Volume fraction of fibers

Subscript

l	lth layer
n	nth layer

Superscript

i	Incident wave field
s	Scattered wave field
r	Refracted wave field
m	Total wave field in the matrix
q_r	Heat flow density in the radial direction
eff	Effective properties of composites

1 Introduction

Composite materials are extensively used in engineering fields for thermal transfer applications. The thermal conductivity is an important property of composites used in electronic packing, thermal insulation, heat spreader, etc. [1]. In order to design and manufacture an optimal material system, the development of micromechanics models to accurately predict the effective thermal conductivity of multiphase composite materials is desirable.

Extensive theoretical and experimental studies on the effective thermal conductivity of a two-phase composite material under different loadings have received great interest in recent years. The methods used to measure the thermal conductivity are divided into two groups: the steady-state and the non-steady-state methods. In the first one, the sample is subjected to a constant heat flow. In the second group, a periodic or transient heat flow is established in the sample [2]. In the past, much attention has been focused on the problems of steady state.

The earliest models for the thermal behavior of composites assumed that the two components are both homogeneous, and are perfectly bounded across a sharp and distinct interface. The Maxwell solution [3] is the starting point to find the effective thermal conductivity of two-phase material systems, but it is only valid for very low concentrations of the dispersed phase. Subsequently, many structural models, e.g., parallel, Maxwell-Eucken [4], and effective medium theory models [5], were proposed. Recently, Samantray et al. [6] applied the unit-cell approach to study the effective thermal conductivity of two-phase materials. Based on an effective medium theory, Bagchi and Nomura [7] developed a theoretical model to predict the effective thermal conductivity of an aligned multi-walled nano-tube polymer composite. The idea of the generalized self-consistent model was also developed by Hashin [8] to determine the effective thermal conductivity of two-phase materials.

In many high-temperature situations, non-steady heat flux is more common. Due to the complexity of non-steady loading, till date, very little work treating the non-steady effective thermal properties has been done. Recently, Monde and Mitsutake [9] proposed a method to determine the thermal diffusivity of solids using an analytical inverse solution for unsteady heat conduction. By using modulated photothermal techniques, Salazar et al. [2] studied the effective thermal diffusivity of composites made of a matrix filled with aligned circular cylinders of a different material. Most recently, Fang and Hu investigated the distribution of dynamic effective thermal properties along the gradation direction of functionally graded materials by using the Fourier heat conduction law [10] and the non-Fourier heat conduction law [11]. Some theoretical attempts addressing the interfacial characteristics between the inclusion and the matrix have been made. Based on an equivalent inclusion concept, Hasselman and Johnson [12] extended Maxwell's theory to systems of spherical inclusion with a contact resistance. Benveniste and his co-workers have proposed several analytical models to predict the effective thermal conductivity of composite materials, which include the important effects of a thermal contact resistance between the fillers and the matrix [13], and the coated cylindrically orthotropic fibers with a prescribed orientation distribution [14].

Nevertheless, little attention has been paid to the non-steady effective thermal conductivity of composites with interfacial layers. With the wide application of functionally graded materials in aerospace and other high-temperature situations, a study on the non-steady effective thermal conductivity of composites with interfacial layers plays a very important role in the design and manufacturing of functionally graded materials.

In this paper, photothermal-wave techniques are applied to predict the non-steady effective thermal conductivity of composites with interfacial layers. Photothermal techniques have become powerful tools for the thermophysical characterization and non-destructive evaluation (NDE) of various materials in the past few decades. First, Ocariz et al. applied the photothermal method to locate and characterize the geometrical and thermal properties of the buried cylinder theoretically [15] and experimentally [16]. Subsequently, Salazar et al. used this method to calculate the in-plane effective thermal diffusivity of unidirectional fiber-reinforced composites [17] and the surface temperature of multilayered cylindrical samples [18]. Salazar et al. [19] also extended this classical flash method to be used with non-planar samples, such as solid cylinders, hollow cylinders, and spheres. Recently, Madariaga and Salazar [20] exploited this elegant method to express the surface temperature of multilayered spherical samples with continuously varying in-depth thermal conductivity. In a series of studies of Wang et al., photothermal radiometry was used for the quantitative NDE of samples with curved surfaces [21], cylindrical composite structures [22], and spherical geometries [23].

The main objective of this paper is to investigate the scattering of thermal waves and the effects of interface layers on the effective thermal conductivity of materials. A thermal wave is often applied with the Fourier conduction law. Fourier's law underlies the "parabolic thermal wave" associated with a non-linear dependence of the thermal conductivity on temperature and the "thermal wave method" of measuring thermal properties. The composite medium contains a random distribution of cylindrical inclusions of the same size with interface layers of the same thickness. The interface layer is modeled by any number of homogeneous layers. The temperature fields in different regions of the material are expressed by using the wave function expansion method, and the expanded mode coefficients are determined by satisfying the boundary conditions at the interfaces. The theory of Waterman and Truell [24] is applied to obtain the non-steady effective thermal conductivity. The effective thermal conductivity under different parameters is graphically illustrated and discussed.

2 Dynamical Equation of Heat Conduction and its Solution

Consider a unidirectional composite material containing long, parallel, randomly distributed cylindrical fibers embedded in an infinite matrix, as depicted in Fig. 1 [25,26]. As is often the case for practical fiber-reinforced plastics, the matrix is assumed to be isotropic and the fibers transversely isotropic, so the resulting unidirectional composite also possesses transverse isotropy. The fibers of radius a_0 have identical properties. Let λ, c, ρ be the thermal conductivity, specific heat capacity, and mass density of the matrix, respectively, and λ_0, c_0, ρ_0 those of the fibers. It is assumed that thick layers

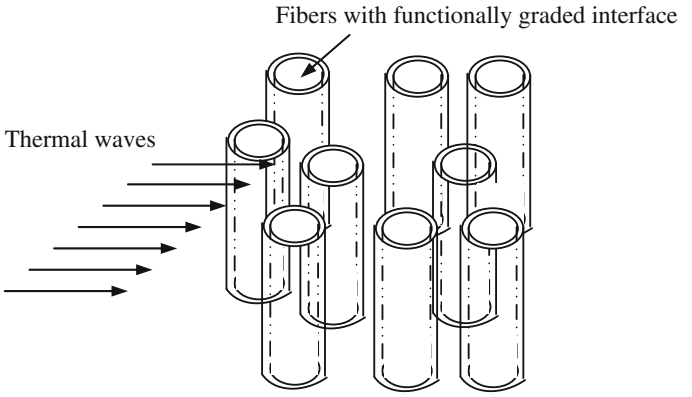

Fig. 1 Unidirectional fiber arrangement in the matrix and the incidence of thermal waves

of uniform thickness h with variable material properties are present at the interfaces separating the matrix from each fiber.

It is assumed that a time-harmonic thermal wave propagates in the direction perpendicular to the reinforcing fibers. In order to study the scattering of thermal waves in a fiber-reinforced composite with interfacial layers, we first consider the scattered field due to a single fiber with an interface layer. Also, let the fiber be separated from the matrix by n layers. The geometry is depicted in Fig. 2, where (x, y) is the Cartesian coordinate system with the origin at the center of the fiber and (r, θ) is the corresponding cylindrical coordinate system. The interface layer is subdivided into several thin cylindrical shells, and the material properties within each shell of inner radius a_{m-1}, outer radius a_m $(m = 1, 2, \ldots, n)$ are λ_m, c_m, ρ_m. The uniform thickness of the shells is $h_m = a_m - a_{m-1}$. Let the boundaries of the fiber and the shells be denoted by C_l $(l = 0, 1, 2, \ldots, n)$.

Based on the Fourier heat conduction law, the heat conduction equation in the composite material, in the absence of heat sources, is described as

$$\nabla^2 T(r, t) = \frac{1}{D}\frac{\partial T}{\partial t}, \tag{1}$$

where $\nabla^2 = \partial^2/\partial x^2 + \partial^2/\partial y^2$ represents the two-dimensional Laplacian operator, T the temperature in the composite materials, and D is the thermal diffusivity with

$$D = \lambda/(\rho c), \tag{2}$$

where λ, c, and ρ are the thermal conductivity, specific heat at constant pressure, and density of the matrix, respectively.

The solution of the periodic steady state is investigated. Suppose that

$$T = T_0 + \mathrm{Re}[\vartheta \exp(-j\omega t)], \tag{3}$$

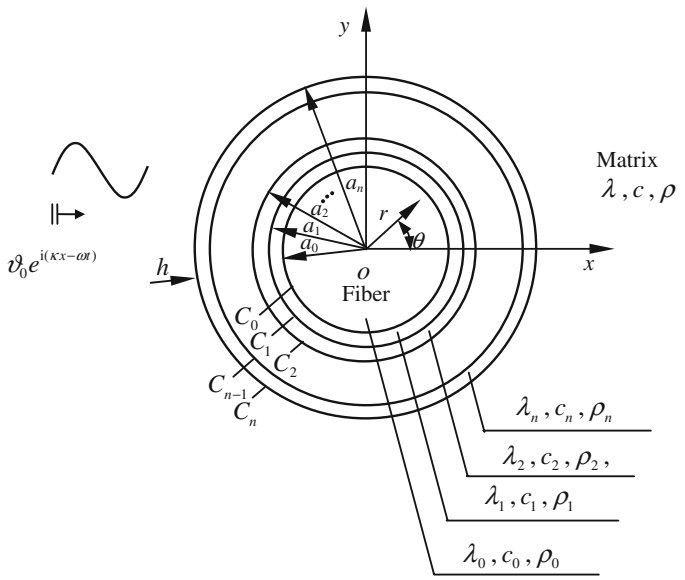

Fig. 2 One cylindrical fiber with interface layers and the layers in composites

where T_0 is the average temperature, ω the incident frequency of thermal waves, j the imaginary unit, and $j^2 = -1$.

Substituting Eq. 3 into Eq. 1, the following equation can be obtained:

$$\nabla^2 \vartheta + \kappa^2 \vartheta = 0, \tag{4}$$

where κ is the wave number of complex variables, and

$$\kappa = (1 + j)k, \tag{5}$$

with $k = \sqrt{\omega/2D}$ being the incident wave number.

By using the wave function expansion method, the incident thermal waves are expressed as

$$\vartheta^{(\mathrm{i})} = \vartheta_0 \mathrm{e}^{j(\kappa x-\omega t)} = \vartheta_0 \sum_{m=-\infty}^{\infty} j^m J_m(\kappa r) \mathrm{e}^{jm\theta} \mathrm{e}^{-j\omega t}, \tag{6}$$

where the superscript (i) stands for the incident waves, ϑ_0 the temperature amplitude of incident thermal waves, and $J_m(\cdot)$ is the mth Bessel functions of the first kind. It should be noted that all wave fields have the same time variation, $\mathrm{e}^{-j\omega t}$, which is omitted in all subsequent representations for notational convenience.

When the thermal waves propagate in the fibrous composite material, the waves are scattered by the fibers, and the scattering waves from the fibers are expanded in a series of outgoing Hankel functions. The scattered field in the matrix is expressed in the form,

$$\vartheta^{(\mathrm{s})} = \sum_{m=-\infty}^{\infty} A_m H_m^{(1)}(\kappa r)\mathrm{e}^{jm\theta}, \tag{7}$$

where the superscript (s) stands for the scattered waves, $H_m^{(1)}(\cdot)$ is the mth Hankel functions of the first kind, and A_m are the mode coefficients that account for the distortion of the scattered cylindrical waves by the fiber.

The total temperature in the matrix should be produced by the superposition of the incident field and the scattered field, i.e.,

$$\vartheta^m = \vartheta^{(\mathrm{i})} + \vartheta^{(\mathrm{s})}. \tag{8}$$

The refracted waves inside the fiber are standing waves, and can be expressed as

$$\vartheta^{\mathrm{r}} = \sum_{m=-\infty}^{\infty} B_m J_m(\kappa_0 r)\mathrm{e}^{jm\theta}, \tag{9}$$

where the superscript r stands for the refracted waves, and B_m are the mode coefficients of refracted waves.

The temperature in the lth layer ϑ^l may be described by the sum of the two components (outgoing and ingoing) and is expressed in the following form [27,28]:

$$\vartheta^l = \left[\sum_{m=-\infty}^{\infty} E_m^l H_m^{(1)}(\kappa_l r)\mathrm{e}^{jm\theta} + \sum_{m=-\infty}^{\infty} F_m^l H_m^{(2)}(\kappa_l r)\mathrm{e}^{jm\theta} \right], \tag{10}$$

where $H_m^{(2)}(\cdot)$ are the mth Hankel functions of the second kind, and denote the ingoing waves, and E_m^l and F_m^l are the mode coefficients in the lth layer.

The wave numbers $\kappa_l$in the $l$thlayer and κ_0 in the cylindrical fiber are given by

$$\kappa_l = (1+j)\sqrt{\omega/2D_l} \quad (l = 1, 2, \ldots, n), \tag{11}$$

$$\kappa_0 = (1+j)\sqrt{\omega/2D_0}, \tag{12}$$

where $D_l = \lambda_l/\rho_l c_l$ and $D_0 = \lambda_0/\rho_0 c_0$.

3 Boundary Conditions and Solution of the Coefficients

The boundary conditions on C_n, C_l, and C_0 are given by

$$\vartheta^n = \vartheta^m, q_{\mathrm{r}}^n = q_{\mathrm{r}}^m \quad \text{for} \quad r = a_n, \tag{13}$$

$$\vartheta^l = \vartheta^{l+1}, q_{\mathrm{r}}^l = q_{\mathrm{r}}^{l+1} \quad \text{for} \quad r = a_l \ (l = 1, 2, \ldots, n-1), \tag{14}$$

$$\vartheta^{\mathrm{r}} = \vartheta^{1}, q_{\mathrm{r}}^{\mathrm{r}} = q_{\mathrm{r}}^{1} \quad \text{for} \quad r = a_0, \tag{15}$$

where q_{r} is the heat flow density in the radial direction, and $q_{\mathrm{r}} = -\lambda \frac{\partial \vartheta}{\partial r}$.

The condition of continuity of temperature on C_n gives

$$\begin{aligned} &\sum_{m=-\infty}^{\infty} \left[E_m^n H_m^{(1)}(\kappa_n a_n) \mathrm{e}^{jm\theta} + F_m^n H_m^{(2)}(\kappa_n a_n) \mathrm{e}^{jm\theta} \right] \\ &= \vartheta_0 \sum_{m=-\infty}^{\infty} j^m J_m(\kappa a_n) \mathrm{e}^{jm\theta} + \sum_{m=-\infty}^{\infty} A_m H_m^{(1)}(\kappa a_n) \mathrm{e}^{jm\theta}. \end{aligned} \tag{16}$$

Multiplying by $\mathrm{e}^{-js\theta}$ and integrating from 0 to 2π, the following equation can be obtained:

$$E_{\mathrm{s}}^n H_{\mathrm{s}}^{(1)}(\kappa_n a_n) + F_{\mathrm{s}}^n H_{\mathrm{s}}^{(2)}(\kappa_n a_n) = \vartheta_0 j^s J_{\mathrm{s}}(\kappa a_n) + A_{\mathrm{s}} H_{\mathrm{s}}^{(1)}(\kappa a_n). \tag{17}$$

The continuous boundary conditions of temperature on C_l and C_0 give

$$E_{\mathrm{s}}^l H_{\mathrm{s}}^{(1)}(\kappa_l a_l) + F_{\mathrm{s}}^l H_{\mathrm{s}}^{(2)}(\kappa_l a_l) = E_{\mathrm{s}}^{l+1} H_{\mathrm{s}}^{(1)}(\kappa_{l+1} a_l) + F_{\mathrm{s}}^{l+1} H_{\mathrm{s}}^{(2)}(\kappa_{l+1} a_l), \tag{18}$$

$$B_{\mathrm{s}} J_{\mathrm{s}}(\kappa_0 a_0) = E_{\mathrm{s}}^1 H_{\mathrm{s}}^{(1)}(\kappa_1 a_0) + F_{\mathrm{s}}^1 H_{\mathrm{s}}^{(2)}(\kappa_1 a_0). \tag{19}$$

According to the continuous boundary conditions of heat flux density on C_n, C_l ($l = 1, 2, \ldots, n-1$) and C_0, one can obtain

$$\begin{aligned} &\lambda_n \left[E_{\mathrm{s}}^n \frac{\partial}{\partial a_n} H_{\mathrm{s}}^{(1)}(\kappa a_n) + F_{\mathrm{s}}^l \frac{\partial}{\partial a_n} H_{\mathrm{s}}^{(2)}(\kappa a_n) \right] \\ &= \lambda \left[A_{\mathrm{s}} \frac{\partial}{\partial a_n} H_{\mathrm{s}}^{(1)}(\kappa a_n) + \vartheta_0 j^{\mathrm{s}} \frac{\partial}{\partial a_n} J_{\mathrm{s}}(\kappa a_n) \right], \end{aligned} \tag{20}$$

$$\begin{aligned} &\lambda_l \left[E_{\mathrm{s}}^l \frac{\partial}{\partial a_l} H_{\mathrm{s}}^{(1)}(\kappa_l a_l) + F_{\mathrm{s}}^l \frac{\partial}{\partial a_l} H_{\mathrm{s}}^{(2)}(\kappa_l a_l) \right] \\ &= \lambda_{l+1} \left[E_{\mathrm{s}}^{l+1} \frac{\partial}{\partial a_{l+1}} H_{\mathrm{s}}^{(1)}(\kappa_{l+1} a_l) + F_{\mathrm{s}}^{l+1} \frac{\partial}{\partial a_{l+1}} H_{\mathrm{s}}^{(2)}(\kappa_{l+1} a_l) \right], \end{aligned} \tag{21}$$

$$\lambda_0 \left[B_{\mathrm{s}} \frac{\partial}{\partial a_0} J_{\mathrm{s}}(\kappa_0 a_0) \right] = \lambda_1 \left[E_{\mathrm{s}}^1 \frac{\partial}{\partial a_0} H_{\mathrm{s}}^{(1)}(\kappa_1 a_0) + F_{\mathrm{s}}^1 \frac{\partial}{\partial a_0} H_{\mathrm{s}}^{(2)}(\kappa_1 a_0) \right]. \tag{22}$$

According to Eqs. 17–22, the expanded coefficient of scattered waves A_{s} can be expressed as

$$A_{\mathrm{s}} = -(P_{\mathrm{s}}/Q_{\mathrm{s}}) \vartheta_0 j^{\mathrm{S}}, \tag{23}$$

where

$$P_{\mathrm{s}} = K_{\mathrm{s}}^{i} - \frac{\lambda}{\lambda_n}(R_{\mathrm{s}}^{n}/T_{\mathrm{s}}^{n})N_{\mathrm{s}}^{i}, \tag{24}$$

$$Q_{\mathrm{s}} = M_{\mathrm{s}} - \frac{\lambda}{\lambda_n}(R_{\mathrm{s}}^{n}/T_{\mathrm{s}}^{n})L_{\mathrm{s}}. \tag{25}$$

The recurrence formulas for R_{s}^{l} and T_{s}^{l} are expressed as

$$R_{\mathrm{s}}^{l}=\frac{K_{\mathrm{s}}^{l}(a_l)-M_{\mathrm{s}}^{l}(a_l)[\lambda_{l-1}K_{\mathrm{s}}^{l}(a_{l-1})-\lambda_l(R_{\mathrm{s}}^{l-1}/T_{\mathrm{s}}^{l-1})N_{\mathrm{s}}^{l}(a_{l-1})]}{[\lambda_{l-1}M_{\mathrm{s}}^{l}(a_{l-1})-\lambda_l(R_{\mathrm{s}}^{l-1}/T_{\mathrm{s}}^{l-1})L_{\mathrm{s}}^{l}(a_{l-1})]} \quad (l=1,2,\ldots,n), \tag{26}$$

$$T_{\mathrm{s}}^{l}=\frac{N_{\mathrm{s}}^{l}(a_l)-L_{\mathrm{s}}^{l}(a_l)[\lambda_{l-1}K_{\mathrm{s}}^{l}(a_{l-1})-\lambda_l(R_{\mathrm{s}}^{l-1}/T_{\mathrm{s}}^{l-1})N_{\mathrm{s}}^{l}(a_{l-1})]}{[\lambda_{l-1}M_{\mathrm{s}}^{l}(a_{l-1})-\lambda_l(R_{\mathrm{s}}^{l-1}/T_{\mathrm{s}}^{l-1})L_{\mathrm{s}}^{l}(a_{l-1})]} \quad (l=1,2,\ldots,n), \tag{27}$$

$$R_{\mathrm{s}}^{0} = J_{\mathrm{s}}(\kappa_0 a_0), \quad T_{\mathrm{s}}^{0} = s J_{\mathrm{s}}(\kappa_0 a_0) - \kappa_0 a_0 J_{\mathrm{s}+1}(\kappa_0 a_0). \tag{28}$$

Note that K_{s}^{i}, N_{s}^{i}, M_{s}, L_{s}, $M_{\mathrm{s}}^{l}(a_l)$, $K_{\mathrm{s}}^{l}(a_l)$, $N_{\mathrm{s}}^{l}(a_l)$, and $L_{\mathrm{s}}^{l}(a_l)$ are given in the Appendix.

4 Effective Propagating Wave Number of Thermal Waves

We now consider a composite material with N fibers randomly distributed in the matrix. Their positions of these fibers are denoted by the random variables ($r_1, r_2, \ldots, r_N$). The total temperature field at any point outside all fibers can be given in the multiple scattering form,

$$\begin{aligned}\vartheta(r; r_1, r_2, \ldots, r_N) = \vartheta^{\mathrm{i}}(r) &+ \sum_{k=1}^{N} T^{\mathrm{s}}\vartheta^{i}(r) \\ &+ \sum_{m=1}^{N} T^{\mathrm{s}}(r_m) \sum_{k=1,k\neq m}^{N} T^{\mathrm{s}}(r_k)\vartheta^{\mathrm{i}}(r) + \cdots,\end{aligned} \tag{29}$$

where the single summation denotes the primary scattered terms, the double summation denotes the secondary terms, and so on. The primary scattering is due to the incident waves alone, and the second scattering represents the rescattering of the primary scattered waves, etc. The multiple scattering theory takes into account the interaction among the distributed fibers accurately. However, it is difficult to deal with in order

to predict the effective properties. Here, we apply the effective field approximation to describe approximately the interaction among the distributed fibers. Following the work of Waterman and Truell [24], the effective propagating wave number can be obtained from the scattered far field.

Once the scattered field due to a single fiber is known, the phase velocities and attenuations of the coherent waves through the composite can be easily calculated by the double plane wave theory of Waterman and Truell [24]. The scattered fields for incident thermal waves at a large distance from the particle can be obtained from Eq. 7 by letting r tend to ∞. After applying the asymptotic expression of the radial function $H_n^{(1)}(\kappa r)$, the scattered wave in the far fields can be expressed asymptotically;

$$\vartheta_r^{(\mathrm{s})} \sim \sqrt{\frac{2}{\pi\kappa r}}\mathrm{e}^{j(\kappa r-\pi/4)}(j\kappa\vartheta_0)f_r(\theta)+o\left(\frac{1}{r}\right), \tag{30}$$

where

$$f_r(\theta)=\sum_{s=-\infty}^{\infty}(-j)^s\frac{A_{\mathrm{s}}}{\vartheta_0}\mathrm{e}^{js\theta}. \tag{31}$$

The function $f_r(\theta)$ is the far-field scattering amplitudes for the scattered thermal waves. It is noted that the far-field scattered amplitudes are dependent on the angle θ. The far-field scattered amplitudes at two specific angles, $\theta=0$ and $\theta=\pi$, are of special interest, and are called the forward and backward scattering amplitudes, respectively.

According to the theory of Waterman and Truell [24], in the case of two-dimensional scatterers, the effective propagating wave number is expressed as

$$\left(\frac{K}{k}\right)^2=\left[1-\frac{2jN}{k^2}f(k,0)\right]^2-\left[\frac{2jN}{k^2}f(k,\pi)\right]^2, \tag{32}$$

where K is the propagating wave number in the effective medium and N is the number of the fibers per unit volume with

$$N=V_{\mathrm{f}}/\pi a_0^2, \tag{33}$$

where V_{f} is the volume fraction of the randomly distributed cylindrical fibers in the matrix.

It is noted that $f(k,0)$ is the forward scattering amplitude of a single scatterer, and $f(k,\pi)$ is the backward scattering amplitude of a single scatterer. In the theory of Waterman and Truell, correlations between the fibers are neglected. Thus, the validity of Eq. 32 is limited to the low volume concentration of fibers.

5 Non-steady Effective Properties of Fiber-Reinforced Composites

According to Eq. 5, the non-steady effective thermal conductivity λ^{eff} in the direction perpendicular to the reinforcing fibers can be easily obtained from the effective prop-

agating wave number as follows:

$$\lambda^{\text{eff}} = \frac{\rho^{\text{eff}} c^{\text{eff}} \lambda}{\rho c} [\text{Re}(k/K)]^2, \tag{34}$$

where $\text{Re}(\cdot)$ denotes the real part, and ρ^{eff} and c^{eff} are the effective mass density and effective heat capacity of composites. From Ref. [9], it is known that ρ^{eff} and c^{eff} always follow the mixture rule, and $\rho^{\text{eff}} c^{\text{eff}}$ is given by

$$\rho^{\text{eff}} c^{\text{eff}} = \rho c \left\{ 1 - V_{\text{f}} \left(1 + \frac{h}{a_0} \right)^2 \right\} + \rho_0 c_0 V_{\text{f}} + \frac{h V_{\text{f}}}{n a_0} \sum_{l=1}^{n} \rho_l c_l \left(2 + \frac{2l-1}{n} \frac{h}{a_0} \right). \tag{35}$$

6 Numerical Examples and Discussion

In the following analysis, it is convenient to make the variables dimensionless. In order to accomplish this step, a representative length scale a_0, where a_0 is the radius of fibers, is introduced. The following dimensionless variables and quantities have been chosen for computation: the incident wave number $k^* = ka_0 = 0.1$–2.0, $h^* = h/a_0 = 0.05$–0.20, $\lambda^* = \lambda_0/\lambda = 2.0$–$8.0$, $c^* = c_0/c = 2.0$–4.0, and $\rho^* = \rho_0/\rho = 2.0$–$4.0$. The dimensionless effective thermal conductivity is $\lambda^* = \lambda^{\text{eff}}/\lambda$.

Specially designed functionally graded interface layers are introduced for a significant improvement of the effective thermal conductivity. The character of the effective thermal conductivity is dependent on the functional form of gradation. In the graded interface layer, the properties are related to the microstructure of two constituents.

Following the work of Sato and Shindo [29], the properties of two special cases of the interface material are considered, and are given by the following equations:

Case I:

$$P_{\text{I}}(r) = \begin{cases} P_0 & (r_i < a_0) \\ (P - P_0) \left(\frac{r - a_0}{h} \right) + P_0 & (a_0 \le r_i \le a_0 + h) \\ P & (r_i > a_0 + h) \end{cases} \tag{36}$$

Case II:

$$P_{\text{II}}(r) = \begin{cases} P_0 & (r_i < a_0) \\ 4(P - P_0) \left(\frac{r - (a_0 + h/2)}{h} \right)^3 + \frac{P + P_0}{2} & (a_0 \le r_i \le a_0 + h) \\ P & (r_i > a_0 + h), \end{cases} \tag{37}$$

where P denotes the properties (thermal conductivity, specific heat, and density) of composites. The material properties of the layers given above are calculated at the midpoint of each layer assuming variations of Cases I and II from the boundary of the inclusion to the matrix medium.

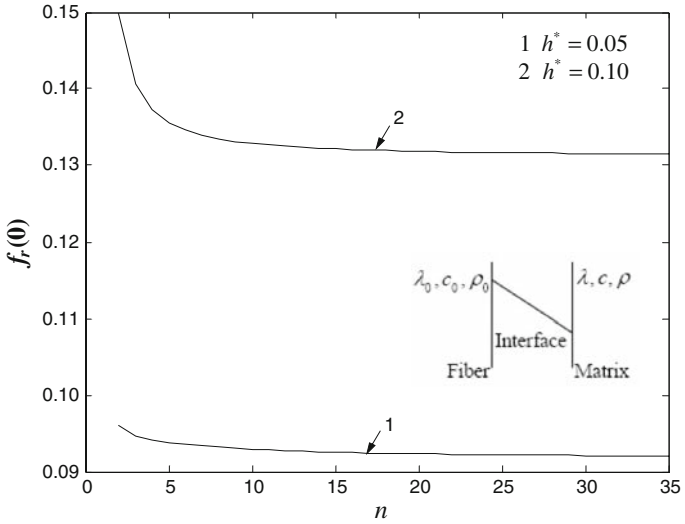

Fig. 3 Far-field scattering amplitudes as a function of the number of layers ($k^* = 1.0, h^* = 0.1, \lambda^* = 4.0, c^* = 2.0, \rho^* = 2.0$)

Figures 3 and 4 show the variation of the far-field scattering amplitudes $f(\kappa, 0)$ for the scattered thermal waves with the number of layers of n for Case I. The scattered waves result from a single fiber. Case I refers to the case of the interface material through which the thermal properties vary linearly from those of the cylindrical fibers to those of the matrix. In Fig. 3, it can be seen that the truncation of n should increase with an increase in the thickness of the interface. The truncation of n at 25 gives adequate results for Case I. Comparing the results in Figs. 3 and 4, it is clear that the truncation of n should increase with an increase in the ratio of the fiber and matrix.

The non-steady effective thermal conductivity of composites as a function of the volume fraction of fibers for Case I with parameters: $k^* = 1.0, \lambda^* = 4.0, c^* = 2.0, \rho^* = 2.0$ is presented in Fig. 5. It can be seen that the non-steady effective thermal conductivity increases with an increase of the thickness of the interface. Because the thermal conductivity of the fiber is greater than that of the matrix, the non-steady effective thermal conductivity increases with the volume fraction of fibers. The effect of the interface on the effective thermal conductivity also increases with the volume fraction of fibers.

Figure 6 illustrates the non-steady effective thermal conductivity as a function of the volume fraction of fibers for Case I with parameters: $V_f = 0.1, \lambda^* = 4.0, c^* = 2.0, \rho^* = 2.0$. It can be seen that the non-steady effective thermal conductivity increases with an increase of the dimensionless wave number, then reaches a maximum and tends to be steady as the wave number increases further. In the region of low frequency, the effect of the interface on the effective thermal conductivity is less than that in the region of high frequency. The maximum effective thermal conductivity increases with the thickness of the interface. The wave number corresponding to the maximum value increases with a decrease in the thickness of the interface.

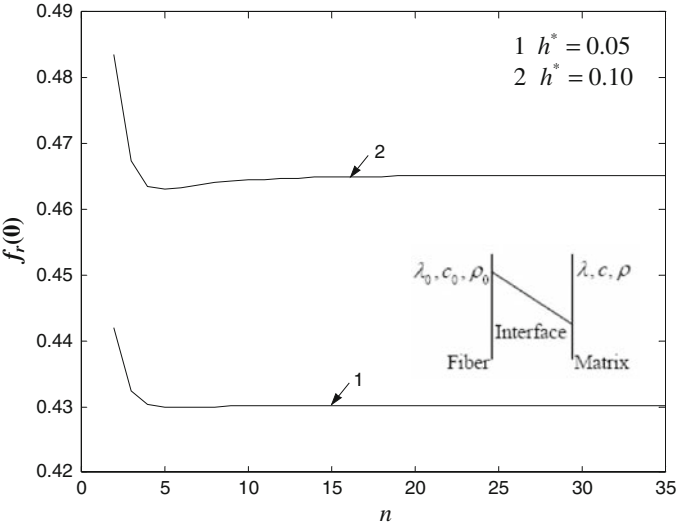

Fig. 4 Far-field scattering amplitudes as a function of the number of layers ($k^* = 1.0$, $h^* = 0.1$, $\lambda^* = 8.0$, $c^* = 2.0$, $\rho^* = 2.0$)

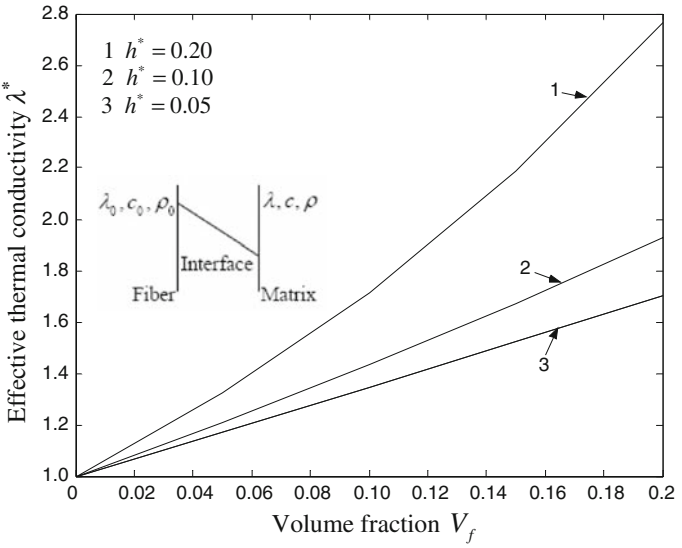

Fig. 5 Non-steady effective thermal conductivity as a function of the volume fraction of fibers ($k^* = 1.0$, $\lambda^* = 4.0$, $c^* = 2.0$, $\rho^* = 2.0$)

Figure 7 illustrates the non-steady effective thermal conductivity as a function of the volume fraction of fibers for Case I with parameters: $V_f = 0.1$, $\lambda^* = 8.0$, $c^* = 2.0$, $\rho^* = 2.0$. It can be seen that the non-steady effective thermal conductivity increases with an increase of the dimensionless wave number, then reaches a maximum and tends to be steady as the wave number further increases. Comparing with the results

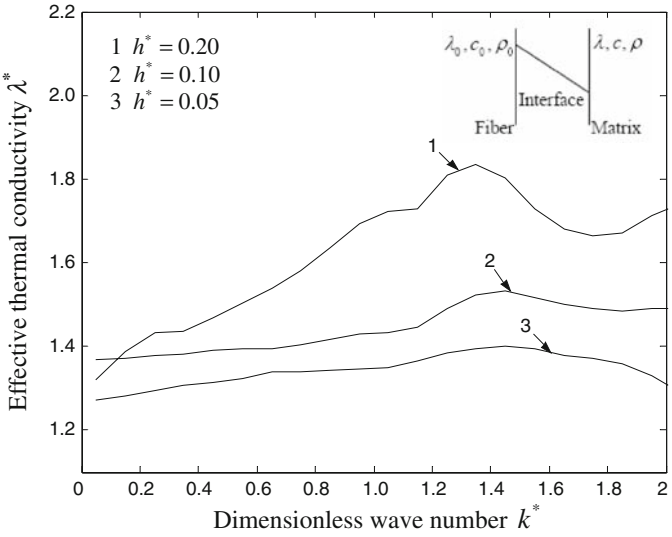

Fig. 6 Non-steady effective thermal conductivity as a function of the dimensionless wave number ($\lambda^* = 4.0$, $c^* = 2.0$, $\rho^* = 2.0$, $V_f = 0.1$)

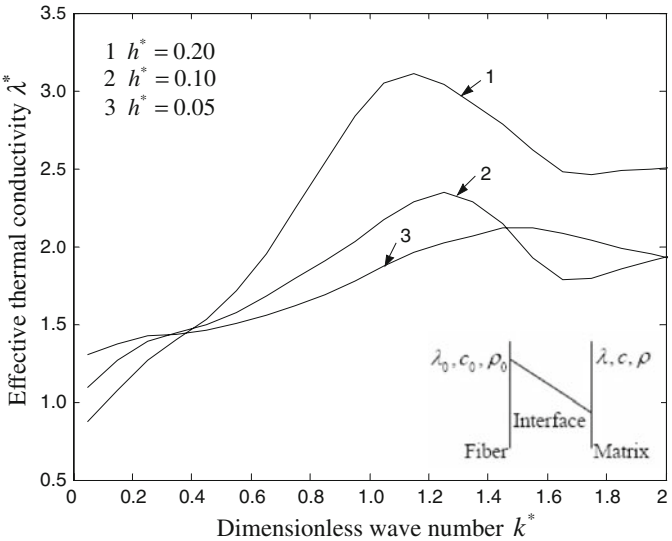

Fig. 7 Non-steady effective thermal conductivity as a function of the dimensionless wave number ($\lambda^* = 8.0$, $c^* = 2.0$, $\rho^* = 2.0$, $V_f = 0.1$)

in Fig. 6, it is clear that the greater the thermal conductivity ratio of the fiber and matrix, the greater the effect of the thickness of the interface on the effective thermal conductivity. In the region of intermediate frequency, the effect of the thickness of the interface on the effective thermal conductivity is greater.

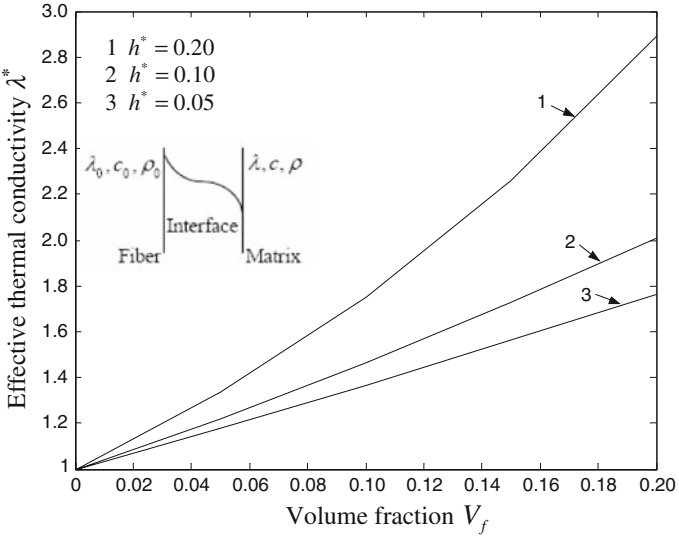

Fig. 8 Non-steady effective thermal conductivity as a function of the volume fraction of fibers ($k^* = 1.0, \lambda^* = 4.0, c^* = 2.0, \rho^* = 2.0$)

The non-steady effective thermal conductivity of composites as a function of the volume fraction of fibers for Case II with parameters: $k^* = 1.0$, $\lambda^* = 4.0$, $c^* = 2.0$, $\rho^* = 2.0$ is presented in Fig. 8. It can be seen that the non-steady effective thermal conductivity increases with an increase in the volume fraction of fibers and the thickness of the interface. Comparing the results in Fig. 5, it is seen that the non-steady effective thermal conductivity in Case I is smaller than that in Case II, especially when the volume fraction of fibers is great.

Figure 9 illustrates the non-steady effective thermal conductivity as a function of the volume fraction of fibers for Case II with parameters: $V_{\mathrm{f}} = 0.1$, $\lambda^* = 4.0$, $c^* = 2.0$, $\rho^* = 2.0$. It can be seen that the non-steady effective thermal conductivity increases with an increase in the dimensionless wave number and the thickness of the interface. When the thickness of the interface is relatively small, the variation of the effective thermal conductivity with the dimensionless wave number is little. Comparing with the results in Fig. 6, it is clear that the variation of the effective thermal conductivity with the dimensionless wave number is less in Case II than that in Case I.

Finally, to demonstrate the validity of this dynamical thermal model, the steady effective thermal conductivity of two-phase composites without an interface is given. As $k^* \to 0$, the dynamic effective thermal conductivity tends to the steady solutions. In Fig. 10, the results obtained from the present model, the effective medium theory [4], and Hasselman and Johnson [12] are plotted. Close agreement is seen to exist between the models at low volume fractions; however, the present model predicts a lower value of the effective thermal conductivity than does the effective medium theory. This is consistent with regard to criticism of the conventional effective medium theory

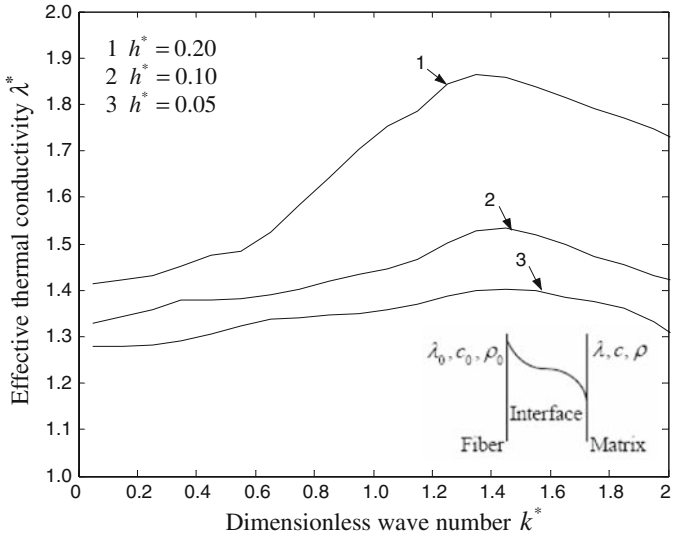

Fig. 9 Non-steady effective thermal conductivity as a function of the dimensionless wave number ($\lambda^* = 4.0$, $c^* = 2.0$, $\rho^* = 2.0$, $V_f = 0.1$)

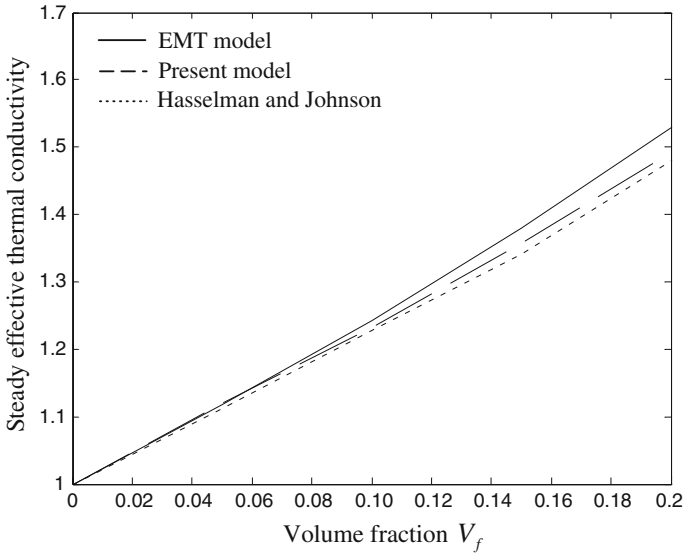

Fig. 10 Comparison of the steady effective thermal conductivity with EMT model and Hasselman and Johnson [12] ($\lambda^* = 4.0$, $c^* = 2.0$, $\rho^* = 2.0$, $h^* = 0$, $k^* = 0$)

for overestimating the effective thermal conductivity of two-phase composites when $\lambda_0 > \lambda$. This is attributed to the assumption that the fibers are regarded as the effective medium even at close range.

7 Conclusions

The scattering of thermal waves in fibrous composites with a functionally grade interface is investigated theoretically by employing a wave function expansion method. The graded interface is divided into a number of layers. The analytical solution of the non-steady effective thermal conductivity of the composite is presented. The theory of Waterman and Truell is applied to obtain the effective propagating wave number of thermal waves. Comparison with the steady effective thermal conductivity demonstrates the validity of the dynamical thermal model.

It has been found that the non-steady effective thermal conductivity of the composites is dependent on the incident wave number, the material properties ratio of the fiber and matrix, and the properties of the interface. The non-steady effective thermal conductivity of the composites increases with an increase in the thickness of the interface, and the thermal conductivity ratio of the fiber and matrix. In contrast to the homogeneous medium, the frequency of the thermal waves has great influence on the effective thermal conductivity. In the region of intermediate frequency, the effects of the thickness of the interface and the thermal conductivity ratio are greater. The effect of the thickness of the interface also shows a significant difference when the volume fraction of fibers varies. Therefore, to gain a high effective thermal conductivity, a greater thickness of the interface layer, a greater thermal conductivity ratio of the fiber and matrix, and intermediate and high frequencies of dynamic loading are preferable.

The results of this paper can provide guidelines for the design of fiber-reinforced composites in the presence of a functionally graded interface and would be helpful in understanding the thermal behavior of composite materials.

Acknowledgment The author is grateful to the anonymous reviewer for his constructive comments and suggestions.

Appendix

The expressions of K_{s}^{i}, N_{s}^{i}, M_{s}, L_{s}, $M_{\mathrm{s}}^{l}(a_l)$, $K_{\mathrm{s}}^{l}(a_l)$, $N_{\mathrm{s}}^{l}(a_l)$, and $L_{\mathrm{s}}^{l}(a_l)$ are given by

$$K_{\mathrm{s}}^{i} = j^{\mathrm{S}} J_{\mathrm{s}}(\kappa a_n), \tag{A1}$$

$$M_{\mathrm{s}} = H_{\mathrm{s}}^{(1)}(\kappa a_n), \tag{A2}$$

$$N_{\mathrm{s}}^{i} = j^{\mathrm{S}}[s J_{\mathrm{s}}(\kappa a_n) - \kappa a_n J_{\mathrm{S}+1}(\kappa a_n)], \tag{A3}$$

$$L_{\mathrm{s}} = s H_{\mathrm{s}}^{(1)}(\kappa a_n) - \kappa a_n H_{\mathrm{S}+1}^{(1)}(\kappa a_n), \tag{A4}$$

$$M_{\mathrm{s}}^{l}(a_l) = H_{\mathrm{s}}^{(1)}(\kappa_l a_l) \quad (l = 1, 2, \ldots, n), \tag{A5}$$

$$K_{\mathrm{s}}^{l}(a_l) = H_{s}^{(2)}(\kappa_l a_l) \quad (l = 1, 2, \ldots, n), \tag{A6}$$

$$N_{\mathrm{s}}^{l}(a_l) = sH_{\mathrm{s}}^{(1)}(\kappa_l a_l) - \kappa_l a_l H_{\mathrm{S}+1}^{(1)}(\kappa_l a_l) \quad (l = 1, 2, \ldots, n), \tag{A7}$$

$$L_{\mathrm{s}}^{l}(a_l) = sH_{\mathrm{s}}^{(2)}(\kappa_l a_l) - \kappa_l a_l H_{\mathrm{S}+1}^{(2)}(\kappa_l a_l) \quad (l = 1, 2, \ldots, n). \tag{A8}$$

References

1. Y. Xu, K. Yagi, Comp. Mater. Sci. **30**, 242 (2004)
2. A. Salazar, J.M. Terrón, A. Sánchez-Lavega, R. Celorrio, Appl. Phys. Lett. **80**, 1903 (2002)
3. J.C. Maxwell, *A Treatise on Electricity and Magnetism*, vol. 1, 3rd edn (Dover, New York, 1954)
4. R.P.A. Rocha, M.E. Cruz, Numer. Heat Transfer A Appl. **39**, 179 (2001)
5. M. Christon, P.J. Burns, R.A. Sommerfeld, Numer. Heat Transfer A Appl. **25**, 259 (1994)
6. P.K. Samantray, P. Karthikeyan, K.S. Reddy, Int. J. Heat Mass Transfer **49**, 4209 (2006)
7. A. Bagchi, S. Nomura, Compos. Sci. Technol. **66**, 1703 (2006)
8. Z. Hashin, J. Compos. Mater. **2**, 284 (1968)
9. M. Monde, Y. Mitsutake, Int. J. Heat Mass Transfer **44**, 3169 (2001)
10. X.-Q. Fang, C. Hu, Comp. Mater. Sci. **42**, 194 (2008)
11. C. Hu, X.-Q. Fang, Thermochim. Acta **464**, 16 (2007)
12. D.H.P. Hasselman, L.F. Johnson, J. Compos. Mater. **21**, 508 (1987)
13. Y. Benveniste, J. Appl. Phys. **61**, 2840 (1987)
14. Y. Benveniste, T. Chen, G.J. Dvorak, J. Appl. Phys. **67,** 2878 (1990)
15. A. Ocariz, A. Sanchez-Lavega, A. Salazar, J. Appl. Phys. **81**, 7552 (1997)
16. A. Ocariz, A. Sanchez-Lavega, A. Salazar, J. Appl. Phys. **81**, 7561 (1997)
17. A. Salazar, A. Sanchez-Lavega, R. Celorrio, J. Appl. Phys. **93**, 4536 (2003)
18. A. Salazar, R. Celorrio, J. Appl. Phys. **100**, 113535 (2006)
19. A. Salazar, F. Garrido, R. Celorrio, J. Appl. Phys. **99**, 066116 (2006)
20. N. Madariaga, A. Salazar, J. Appl. Phys. **101**, 103534 (2007)
21. C. Wang, A. Mandelis, Y. Liu, J. Appl. Phys. **96**, 3756 (2004)
22. C. Wang, A. Mandelis, Y. Liu, J. Appl. Phys. **97**, 014911 (2005)
23. C. Wang, Y. Liu, A. Mandelis, J. Shen, J. Appl. Phys. **101**, 083503 (2007)
24. P.C. Waterman, R. Truell, J. Math. Phys. **2**, 512 (1961)
25. Z. Hashin, P.J.M. Monteiro, Cement Concrete Res. **32**, 1291 (2002)
26. H. Nozaki, Y. Shindo, Int. J. Eng. Sci. **36**, 383 (1998)
27. J. Sinai, R.C. Waag, J. Acoust. Soc. Am. **83**, 1728 (1988)
28. Y.-S. Joo, J.-G. Ih, M.-S. Choi, J. Acoust. Soc. Am. **103**, 900 (1998)
29. H. Sato, Y.Shindo, Int. J. Solids Struct. **38**, 2549 (2001)